2022

Variable Mixing Chamber Waste-Heat Driven Ejector Cycle For Commercial Refrigeration

Egoi Ortego Sampedro

Variable mixing chamber waste-heat driven ejector cycle for commercial refrigeration

Egoi ORTEGO SAMPEDRO[1]*

Mines Paris PSL, Centre d'Efficacité Energétique des Systèmes
Palaiseau, France
egoi.ortego@minesparis.psl.eu

ABSTRACT

Ejectors are commonly studied for heat-driven refrigeration systems. Constant mixing area ejectors are limited in cooling capacity because of the presence of a shocked flow in the mixing chamber in normal conditions. Besides, this geometric constraint makes ejectors extremely sensitive to the outlet pressure variations usually associated with ambient temperature variations; at high temperatures, ejectors can suddenly stall leading to zero power. The author developed a variable mixing chamber ejector concept that helps in reducing the drawbacks of ejectors. It makes it possible to increase the mixing chamber cross-sectional area at moderate temperatures and reduce it at high temperatures. This results in an extended range of operation. In this paper, the benefits of using this new ejector as a heat-driven compressor booster stage are quantified. The ejector-based booster stage can be driven by low grade heat or solar power. The variable mixing chamber ejector opening is adapted to the condensation temperature to maximize the entrained flow rate for every operating condition; this maximizes the cooling capacity whatever the condensation temperature is. New system architecture for commercial refrigeration is explored in the paper. The gains are computed by common thermodynamic models and a specific ejector reduced model derived from CFD modeling. The refrigeration efficiency gains of the studied architectures are compared to a classical vapor compression refrigeration system.

1. INTRODUCTION

Increasing air conditioning and cooling needs will certainly participate to the future issues on energy distribution systems. Cold power production using industrial waste heat is a promising solution to reduce these needs. Especially heat-driven ejector cooling systems should increase in popularity thanks to their relative simplicity and reliability. However, the operational non-flexibility of ejectors is still a limiting factor. One solution is to use hybrid systems based on combinations of ejectors and compressors. This solution has been tested for example by (Wang, Cai, Wang, Yan, & Wang, 2016) where the hybrid system performance was compared to a standard Vapor Compression Cycle (VCC). The compressor was placed at the ejector secondary inlet in the cited study. The performance evaluation was conducted for the R134a refrigerant, at evaporation temperatures between -4°C and 11°C (2.5bar to 4.3bar) for various primary pressures. The gain in COP compared to the VCC at 35.5°C condensing temperature was 74% and 55% for the evaporation temperatures mentioned before. The reference COP at 11°C evaporation temperature was 2.3 which is relatively low. Another example is the theoretical work by (Yoshida & Elbel, 2021) where a compressor was placed at the ejector secondary inlet. The refrigeration fluid was R1234ze(E) which has thermodynamic properties very close to R134a. At condensing temperatures of 20°C and 35°C, for an evaporation temperature of 5°C, the gain in COP was 63% and 6% for mentioned condensing temperatures. The nominal COP of the VCC was 5.7 for 35°C condensation temperature.

The potential gains using such systems are very promising. However, the number of studies on this topic is relatively few. Furthermore, the use of fixed geometry ejectors limits the flexibility and cooling capacity of ejectors. In this paper the potential of a new variable mixing chamber ejector is analyzed for waste-heat driven commercial cold power production. This kind of ejector maximizes the attainable entrained flow rate for every ejector outlet pressure. The entrained flow rate can be increased up to 120% at moderate outlet pressures and the critical pressure can considerably be increased (Ortego Sampedro, 2022).

2. SYSTEM & COMPONENETS DESCRIPTION

The studied variable mixing chamber ejector was presented by the author in a precedent work (Ortego Sampedro, 2022); it was named range extended ejector (RE ejector). This ejector allows maximizing the cooling power for every outlet pressure by adapting the cross section of the mixing chamber. This can be done at constant motive nozzle inlet conditions so at constant motive flow rate. The mixing chamber cross sectional area is reduced at high outlet pressures and increased at low pressures. This allows a significant increase of the ejector efficiency. **Figure *1***gives the primary and entrained flow rates profile in function of condensation temperature. This is a plot derived from the numerical analysis presented in (Ortego Sampedro, 2022). The entrained flow rates were given for a standard ejector and for a RE ejector. The first had a mixing to throat section ratio of 5.76 and the last any value between 3.8 and 10.6.

This ejector was studied for a 10°C evaporation cold power production using industrial waste-heat. In order to lower the operational evaporation temperature, a hybrid system is studied here where the heat-driven system is associated to various compressors. The system is presented in **Figure *2***. Compressors 1 and 2 operate in series; the main operating particularity here is that compressor 2 operates at variable flow rate. The flow leaving compressor 1 passes partly in compressor 2 and partly in RE ejector. The flow passing through compressor 2 will be minimized for each condensation pressure thanks to the RE ejector adaptation. In **Figure *2*** the working fluid circuits are represented in two colors in order show the architecture of what could be a classical VCC (in black) and what could be the a part of a classical heat-driven ejector refrigeration cycle (in blue).

The new architecture performance will be compared to the VCC performance.

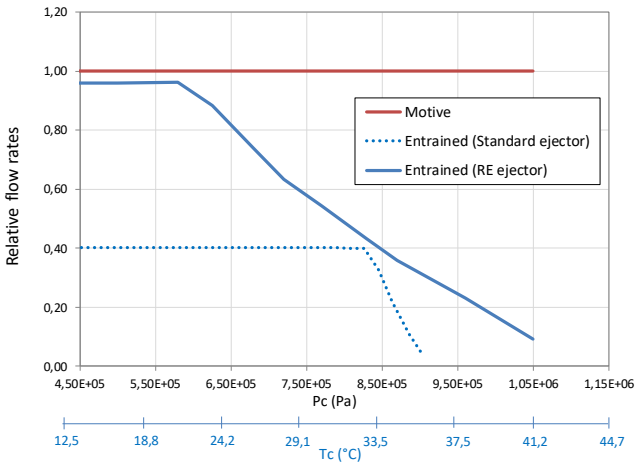

Figure 1: motive and entrained flow rates for standard and RE ejectors (Ortego Sampedro, 2022)

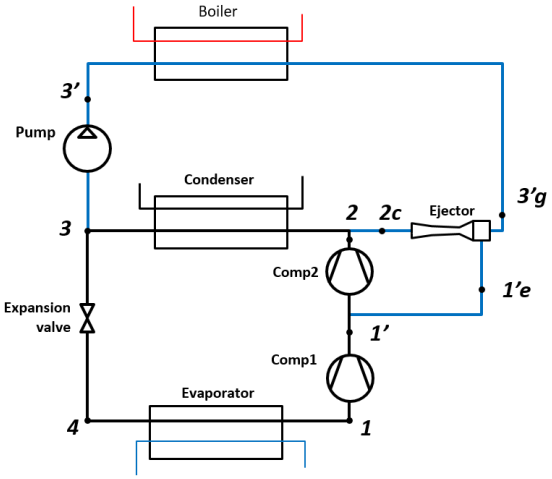

Figure 2: ejector booster refrigeration system

3. METHODS

3.1 Operating conditions

The hybrid system will be evaluated at an evaporation temperature of -10°C which corresponds to a usual value for commercial refrigeration. The nominal condensation temperature is set to 31°C.

The outlet pressure of compressor 1 ($P_{1'e}$) is limited here by the maximum compression ratio selected for compressor 1. For this preliminary study it was decided that the compression ratios of the two compressors would be similar at the nominal design point of the cycle. Given the nominal evaporator and condenser saturation temperatures the maximal value for $P_{1'e}$ is then set to 4bar.

For seasonal variation simulations, $P_{1'e}$ is reduced compared to the nominal if the condensation temperature drops below its nominal value. The lower limit for $P_{1'e}$ was set equal to the evaporation pressure. When $P_{1'e}$ has a value between its minimum and 4bar, it takes a value so the compression ratio of the ejector is maintained at a value that allows maximizing its entrainment ratio. It was verified by CFD computations that a compression ratio of 1.4

satisfies this condition. These CFD calculations were also used to extend the data set available to model the ejector performance. This data set and the reduced model of the ejector are presented in the next section.

The operating conditions are summarized in **Table *1***.

Table 1: operating conditions

Evaporation temperature (°C)	-10
Condensing temperature (°C)	20 to 40
$P_{1,e}\ (bar)$	3 to 4.1
$P_{3,g}\ (bar)$	28.7
$T_{3,g}\ (°C)$	94°C

The compressor 1 inlet superheat is fixed to 5K. The condenser outlet sub-cooling to 2K. Compressors isentropic efficiency was assumed to be 70% and the pump efficiency 70%.

The condensation temperature is defined in function of the ambient temperature at the considered geographic location. A temperature difference of 5K is assumed between ambient and condensation temperatures.

3.1 Ejector description and performance

The range extended ejector CFD initial evaluation was done using R134a (Ortego Sampedro, 2022). That evaluation was done for a specific literature geometry by (Valle, Jabardo, Ruiz, & Alonso, 2014) modified following the original principle of lateral movable slots called also ‘’range extender’’. Figure 3 shows the internal geometry of the modified ejector for two positions of range extender; it can increase or decrease the effective cross sectional area of the mixing chamber.

The RE ejector performance was evaluated for an evaporation temperature of 10°C (4bar saturation pressure) for condensation temperatures ranging from 15°C to 43°C and for a boiler saturation temperature of 84.4°C. Static pressures were set for all boundaries; static temperatures were set also for the two inlets. The CFD computations configuration details are available in (Ortego Sampedro, 2022).

The simulations were performed for 10 positions of the range extender; mass flow rates at the primary and secondary were obtained for a series of outlet pressures. Figure 4 gives the resulting entrainment ratios. The position of the range extender is given in millimeters; 0mm is the normal or initial position, negative indicates a closing and positive an opening. The yellow dots are the reference points identified as critical points for each position; they are used to build the reduced model. The junction of these points corresponds to the entrained flow rate curve in **Figure *1*** (solid blue line in **Figure *1***). This gives the general operating curve of the range extended ejector for a given set of inlet conditions at the primary and the secondary. The opening of the range extender is adapted in function of the outlet pressure.

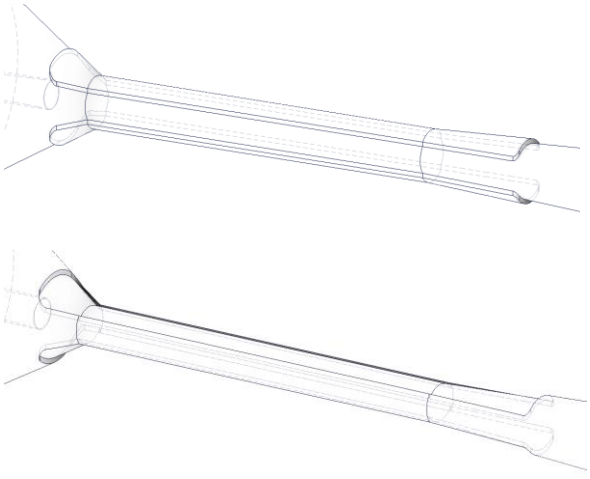

Figure 3: internal volume of the modified ejector: upper: 0.5mm opened extender; lower: 0.5mm closed extender

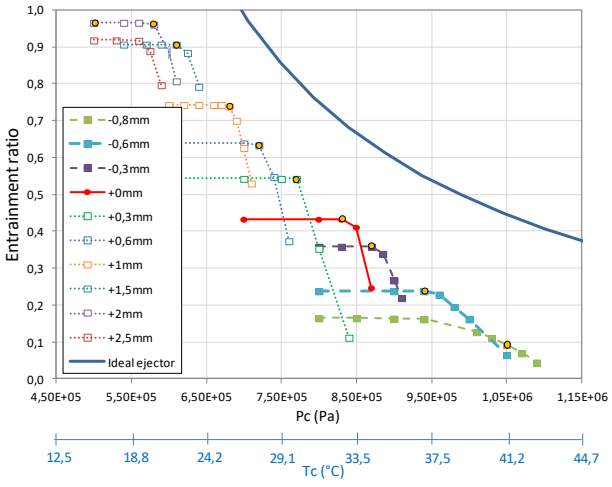

Figure 4: entrainment ratio function of outlet pressure the corresponding condensation temperature;$T_{sat\ 3,g}$ = 84,4°C; $T_{sat\ 1,e}$ = 10°C; 10 extender positions

The reduced model giving the entrained flow rate is defined as follows:

$$\dot{m}_{1'e}(P_{2c}) = \begin{cases} \dot{m}_1 & for\ P_{1'} < P_{2c} < P_{tr} \\ \dot{m}_1\ g(P_{2c}) & for\ P_{tr} < P_{2c} \end{cases} \quad (1)$$

This formulation defines the entrained flow rate as a function of a reference flow rate, an entrainment ratio function (g), the condensation pressure (P_{2c}) and a transition pressure (P_{tr}). The reference flow rate is also the maximal. It is assumed here that the maximal flow rate is equal to the compressor 1 flow rate ($\dot{m}_1$) for the nominal intermediate pressure of 4bar.

The transition condensation pressure (P_{tr}) was 5.8bar is the case of the RE ejector studied here (see **Figure *1***). Bellow the pressure P_{tr} the mass flow rate is constant, above P_{tr} it is multiplied by g that gives values between 0 and 1. In consequence, the suction flow rate is decreasing with increasing pressure if higher than P_{tr} ; this is a classical behavior of ejector. The difference here is that this reduction curve is made by an infinite series of critical points whereas in classical ejectors the decrease is related to a stall and is much ruder. For more detailed physical insight on this aspects please refer to (Ortego Sampedro, 2022).

Function g was defined by fitting a second order polynomial to the data obtained in the above mentioned numerical study (Ortego Sampedro, 2022).

$$g(T_c) = A + B\ P_{2c} + B\ {P_{2c}}^2 \quad (2)$$

The operating conditions are unchanged at the primary for the present study. However, the conditions at the secondary may change. This is due to the system control strategy that is presented is the precedent section.

For intermediate pressures ($P_{1'e}$) below the nominal, the ejector is operated at a low compression ratio as explained before i.e. 1.4. In that situation the entrainment ratio does not change with condensation pressure, it only changes with intermediate pressure.

In order to include this situation in the reduced model, three supplementary conditions at the ejector entrainment inlet were simulated by CFD for the position of the range extender giving the highest entrainment ratio (+2mm). For the ejector outlet, a series of pressures were set in order to verify that the entrainment ratio was independent to P_{2c}. They ranged from 1 to 1.4 times $P_{1'e}$. Table 2 gives the set of new operating conditions simulated specifically for this work. The table gives the maximal entrainment ratios obtained by CFD. These points complete the data set obtained in (Ortego Sampedro, 2022).

Table 2: effect of $P_{1'e}$ *on the maximal entrainement ratio*

		$P_{1'e}$ (bar)		
		3	3.5	4
$P_{2c}/P_{1'e}$	1	0.69	0.81	0.96
	1.4	0.69	0.81	0.96

Reading this table, one observes that when $P_{1'e}$ drops below the nominal, since the entrained gas density drops, the entrained mass flow rate decreases. It is a linear function of the actual to nominal density ratio.

3.3 System modeling

As mentioned above the reference system is a VCC system. The cooling efficiency is computed by the following equation. It gives the ratio between the cooling capacity and the compressor power.

$$EER_{VCC} = \frac{h_1 - h_4}{h_2 - h_1} \quad (3)$$

For the VCC, the two compressors operate at exactly the same flow rate.

For the hybrid system (hy), the cooling efficiency depends on the flow rate passing thought each component as described by the following equation.

$$EER_{hy} = \frac{\dot{m}_1(h_1 - h_4)}{\dot{m}_1(h_{1'} - h_1) + \dot{m}_2(h_2 - h_{1'}) + \dot{m}_{3'}(h_{3'} - h_3)} \quad (4)$$

The flow rate of compressor 2 depends on the flow rate entrained by the ejector ($\dot{m}_{1'e}$) as follows:

$$\dot{m}_2(T_c) = \dot{m}_1 - \dot{m}_{1'e}(T_c) \quad (5)$$

The effect of flow rate variation of compressor 2 on its efficiency is not modeled.

As a complement of the EER, the thermal efficiency (EER_{th}) was evaluated. It is defined as the ratio between the cooling capacity ($\dot{Q}_h$) to the heat required in the boiler ($\dot{Q}_c$). The flow rate in the boiler ($\dot{m}_{3'}$) is constant.

$$EER_{th} = \frac{\dot{Q}_c}{\dot{Q}_h} = \frac{\dot{m}_1(h_1 - h_4)}{\dot{m}_{3'}(h_{3'g} - h_{3'})} \quad (6)$$

Flow rate $\dot{m}_{3'}$ is equal to the maximal entrained flow rate divided by the maximal entrainment ratio as expressed by equation 7. The flow rate $\dot{m}_1$ can thus be simplified in equation 6.

$$\dot{m}_{3'} = \frac{\dot{m}_1}{\mu_0} \quad (7)$$

The maximal entrainment ratios (μ_0) were reported in Table 2. They are only a function of $P_{1'e}$.

4. RESULTS

4.1 Performance comparison

Figure *5* gives the EER of the VCC system and the hybrid system as function of the condensation temperature for evaporation temperatures of -10°C. The hybrid system performance is always higher than the VCC performance. The improvement is higher for lower condensation temperatures. This is related to an increasing entrained flow rate when the compression ratio of the upper stage reduces. This has a direct effect on the power consumption of the compressors.

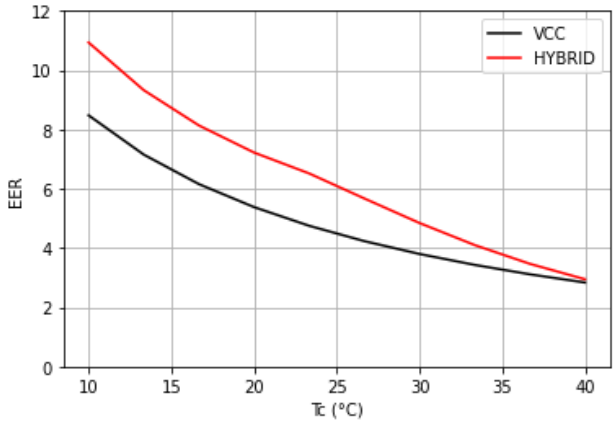

Figure 5: EER function of Tc at Te=-10°C

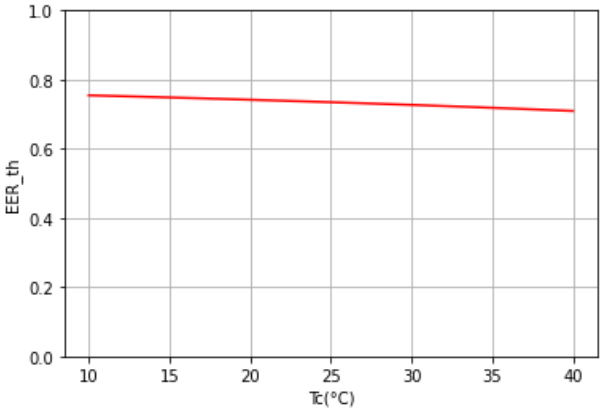

Figure 6: hybrid system EER_{th} function of Tc at Te=-10°

The EER_{th} is shown by **Figure *6***. It is around 0.7. Its value is almost constant; this is related to the hybridization. Its high value is related to the variable mixing chamber solution that allows operating at very high entrainment ratios whatever the Tc value is. Furthermore, this is achieved with a constant primary flow rate.

4.2 Seasonal performance comparison

4.2.1. Efficiencies

The seasonal performance was evaluated assuming constant cold capacity needs. It was done for monthly average temperatures of Tokyo and Los Angeles in 2019 reported in (Yoshida & Elbel, 2021). **Figure *7*** and **Figure *8*** give the monthly average EER for both VCC and hybrid systems. As expected the EER is very sensitive to the ambient temperature; this is in particular visible for Tokyo. The hybrid system has a better EER in all the cases. The thermal EER was not show here since its dependence in regard to the ambient temperature is very small.

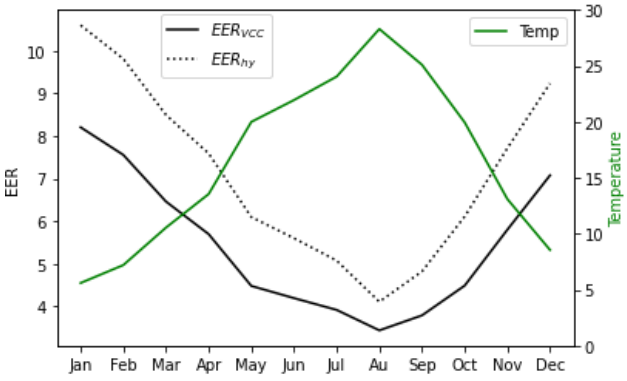

Figure 7: monthly EER and average temperatures; Tokyo

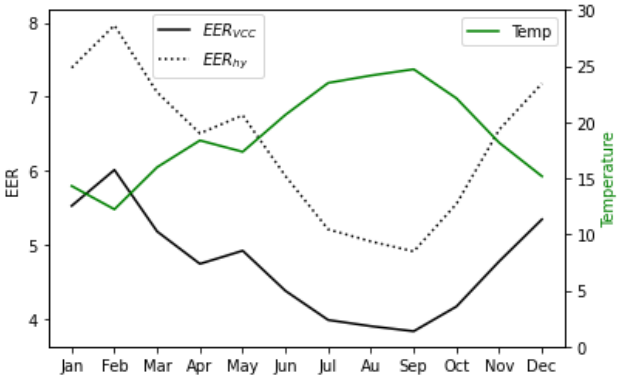

Figure 8: monthly EER and average temperatures; Los Angeles

Table *3* gives the annual average EER and EERth. These are simple arithmetic averages since the cooling capacity was assumed to be constant for all months. The gain in EER is around 30% for the two locations. The average EER_{th} is 0.74 for the hybrid system.

Table 3: annual averages

	T_av(°C)	EER_{VCC}	EER_{hy}	EER_{th}
Tokyo	16.5	5.42	7.11 (+31%)	0.74
Los Angeles	18.9	4.73	6.34 (+34%)	0.74

4.2.2. Operating parameters

In order to give a supplementary insight on the advantage of using a variable geometry ejector the operating pressures (**Figure *9***) and the electrical power consumed per unit cold capacity (**Figure *10***) are presented below for Tokyo. The pressure ratio applied on compressor 2 ranges between 1.4 and 2; it is similar to the one of the compressor 1. However, the compressor 2 power has very low values; even during the hottest month, its power is only 60% of the compressor 1 power. This is possible since the Range Extended ejector operates at high entrained flow rates during cold months and attains high compression ratios during summer months.

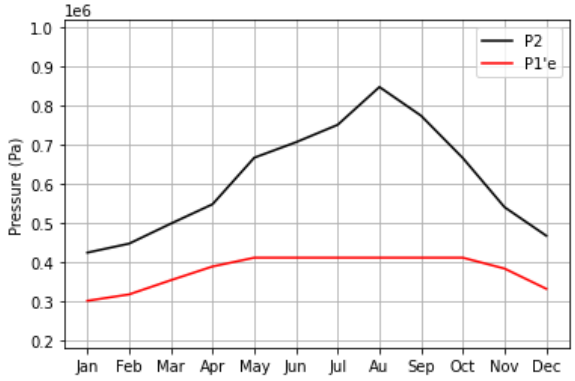

Figure 9: monthly operating pressures; Tokyo

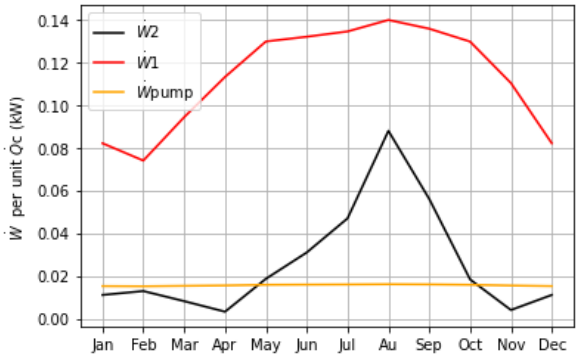

Figure 10: monthly specific powers; Tokyo

6. CONCLUSIONS

A preliminary theoretical study was conducted to assess the performance of a variable mixing chamber ejector based hybrid refrigeration system driven by waste heat and compressors. The specificity of the new tested ejector is its extended high efficiency operating range that allows maximizing the entrained flow rate for every ejector outlet pressures. The ejector is coupled to a variable flow compressor in the hybrid system.

The annual performance of the hybrid system was compared to the one of a simple vapor compression cycle. At an evaporation temperature of -10°C, the hybrid system presents a seasonal EER 30% higher than the VCC system. The seasonal EERth of the hybrid system is 0.74.

The next step would be to define an optimized initial sizing of the ejector and an optimal intermediate pressure for a specific set of meteorological data. Including the real cooling capacity needs could also further enrich the analysis.

NOMENCLATURE

EER	energy efficiency ratio	
g	entrainment ratio function	
h	specific enthalpy	J/kg
$\dot{m}$	mass flow rate	kg/s
P	pressure	Pa
$\dot{Q}$	thermal power	W
T	temperature	K
VCC	vapor compression cycle	
$\dot{W}$	mechanical power	W
μ	entrainment ratio	

Subscript

c	condensation
e	evaporation
th	thermal

REFERENCES

Ortego Sampedro, E. (2022). A new variable mixing chamber ejector: CFD assessment. *Applied Thermal Engineering , 208*.

Valle, J. G., Jabardo, J. S., Ruiz, F. C., & Alonso, J. S. (2014). An experimental investigation of a R-134a ejector refrigeration system. *International journal of refrigeration , 46*, 105-113.

Wang, H., Cai, W., Wang, Y., Yan, J., & Wang, L. (2016). Experimental study of the behavior of a hybrid ejector-based air-conditioning system with R134a. *Energy Conversion and Management* , 31-40.

Yoshida, T., & Elbel, S. (2021). Numerical Analysis For Performance Comparison Between HybridNumerical Analysis For Performance Comparison Between Hybrid Ejector And Conventional Refrigeration SystemsEjector And Conventional Refrigeration Systems. *International Refrigeration and Air Conditioning Conference, Purdue.* West Lafayette.